SALS: Sparse Attention in Latent Space for KV cache Compression

Junlin Mu[1,2,3,*], **Hantao Huang**[3,†], **Jihang Zhang**[3], **Minghui Yu**[3,†], **Tao Wang**[1,2,†], **Yidong Li**[1,2,†]
[1]Key Laboratory of Big Data & Artificial Intelligence in Transportation, Ministry of Education, China
[2]School of Computer Science & Technology, Beijing Jiaotong University, China
[3]ByteDance Seed, China

Abstract

Large Language Models (LLMs) capable of handling extended contexts are in high demand, yet their inference remains challenging due to substantial Key-Value (KV) cache size and high memory bandwidth requirements. Previous research has demonstrated that KV cache exhibits low-rank characteristics within the hidden dimension, suggesting the potential for effective compression. However, due to the widely adopted Rotary Position Embedding (RoPE) mechanism in modern LLMs, naive low-rank compression suffers severe accuracy degradation or creates a new speed bottleneck, as the low-rank cache must first be reconstructed in order to apply RoPE. In this paper, we introduce two key insights: first, the application of RoPE to the key vectors increases their variance, which in turn results in a higher rank; second, after the key vectors are transformed into the latent space, they largely maintain their representation across most layers. Based on these insights, we propose the Sparse Attention in Latent Space (SALS) framework. SALS projects the KV cache into a compact latent space via low-rank projection, and performs sparse token selection using RoPE-free query–key interactions in this space. By reconstructing only a small subset of important tokens, it avoids the overhead of full KV cache reconstruction. We comprehensively evaluate SALS on various tasks using two large-scale models: LLaMA2-7b-chat and Mistral-7b, and additionally verify its scalability on the RULER-128k benchmark with LLaMA3.1-8B-Instruct. Experimental results demonstrate that SALS achieves SOTA performance by maintaining competitive accuracy. Under different settings, SALS achieves 6.4-fold KV cache compression and 5.7-fold speed-up in the attention operator compared to FlashAttention2 on the 4K sequence. For the end-to-end throughput performance, we achieves 1.4-fold and 4.5-fold improvement compared to GPT-fast on 4k and 32K sequences, respectively. The source code will be publicly available in the future.

1 Introduction

The groundbreaking success of Large Language Models (LLMs), such as ChatGPT [15] and Claude [1], is transforming information retrieval in many areas. The exponential growth in LLM service requests is creating an unprecedented demand for inference optimization algorithms, especially for long-context applications. In particular, many research efforts [14, 20, 28, 33] show that the Key-Value cache (KV cache) acts as a major performance bottleneck in LLM serving. As the sequence length increases, the KV cache consumes a large portion of GPU device memory. This

[*]Work done at ByteDance
[†]Corresponding authors.twang@bjtu.edu.cn,{huanghantao,yuminghui.exp}@bytedance.com,ydli@bjtu.edu.cn

39th Conference on Neural Information Processing Systems (NeurIPS 2025).

Table 1: KV data movement, memory cost and complexity comparison of quantization, low rank and token sparse method that is with fixed, dynamic and local token selection strategy.

Name	Methods	KV data movement	Memory size	Computation Complexity	Accuracy
Palu [4]	Low Rank	Median	Low	High	Low
Loki [20]	Dynamic + Low Rank	Low	Median	Median	Median
StreamingLLM [33]	Fixed pattern	Low	Median	Low	Low
Quest [22]	Dynamic	Low	High	Median	Median
DS [29]	Dynamic	Low	Median	Median	High
Hshare [25]	Dynamic	Low	Median	Median	High
SALS (Ours)	Dynamic+Low Rank	Low	Low	Midian	High

high resource requirement underscores the urgent need to mitigate the KV cache memory overhead and further improve attention efficiency.

To tackle the KV cache overhead challenge, previous works [4, 20] show that the KV cache exhibits low-rank characteristics within the hidden dimension, and thus can be effectively compressed in the latent space. Palu [4] further shows that there exists a clear trade-off between accuracy and reconstruction overhead for multi-head attention. Compressing each KV head separately reduces the overhead but at the cost of losing accuracy. However, compressing all heads together by low-rank projection improves accuracy by preserving the global information but results in significantly increased reconstruction cost. In this work, we show that sparsely selecting a small subset of tokens from the KV cache significantly reduces reconstruction error while preserving model accuracy.

Recently, Rotary Position Embedding (RoPE) [21] has been widely adopted in LLMs; it introduces sinusoidal positional information by multiplying query and key states with rotation matrices. This not only prevents the fusion of low rank weights into the query state, but also requires the reconstruction of key states from the latent space. In this work, we observe that the application of RoPE to the key vectors increases their variance, which in turn results in a higher rank. Therefore, the KV cache must be compressed before applying RoPE, which leads to high reconstruction complexity. We further observe that the key vectors in the latent space largely preserve their representation across most layers. Inspired by Double Sparse [29], we use these compressed key vectors as token selection guidance, so that only the selected tokens need to be reconstructed, which significantly reduces the reconstruction complexity.

In this paper, we propose the Sparse Attention in Latent Space (SALS) framework. SALS projects all attention heads into a shared single-head latent space via low-rank projection, for both pre-RoPE queries and pre-RoPE keys. The approximation attention scores are computed in the latent space and the top-k tokens are selected accordingly. These selected tokens are then reconstructed and applied with RoPE for the final attention computation. By reconstructing only a small subset of all tokens, it avoids the overhead of full KV cache reconstruction.

In summary this paper makes the contributions as follow:

- We observe that applying RoPE to key vectors leads to increased variance, resulting in higher rank and lower compression rates. In , key vectors before RoPE can still maintain the representation for the critical token selection.
- We propose the Sparse Attention in Latent Space (SALS) framework to utilize the low-rank pre-ROPE KV cache compression and further to adopt the KV cache in latent space to select critical tokens. The sparse attention is then proposed with reduced KV data movement and computational complexity.
- We comprehensively evaluate SALS on various tasks using two large-scale models: LLaMA2-7b-chat and Mistral-7b, and additionally verify its scalability on the RULER-128k benchmark with LLaMA3.1-8B-Instruct. Experimental results show that we can achieves much higher accuracy comparing to the low-rank based KV cache compression. Comparing to sparse attention works, under the similar benchmark accuracy, SALS achieves 6.4-fold KV cache compression and 5.7-fold speed-up in attention operator compared to FlashAttention2 on 4K sequence. For the end-to-end throughput performance, SALS achieves 1.4-fold and 4.5-fold improvement compared to GPT-fast on 4k and 32K sequences respectively.

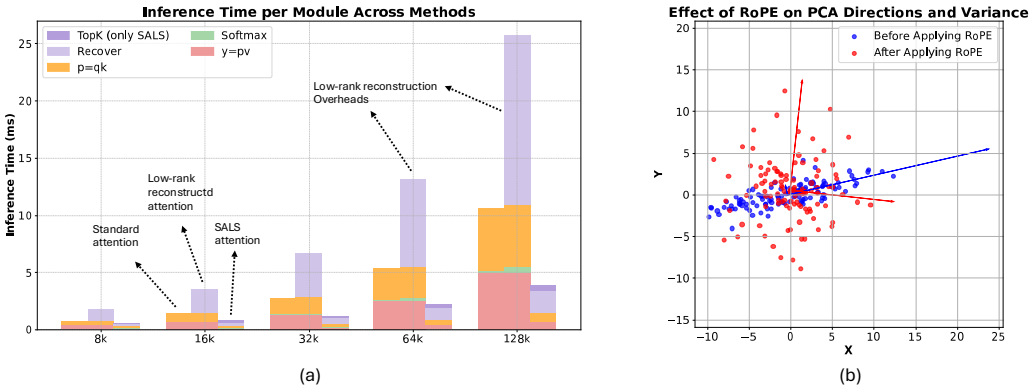

Figure 1: (a) Increasing inference time due to low-rank matrix reconstruction. Low-rank KV cache with overhead leads to longer inference time than the standard attention due to the reconstruction overhead; (b) A simplifed key vector example with changed PCA direction after applying RoPE

2 Related work

2.1 Attention in Latent Space

The low rank matrix decomposition such as singular value decomposition (SVD) to compress LLMs has been actively studied. Existing works such as ASVD [31], SVD-LLM [24] and CALDERA [18] are proposed to compress LLM weights. However, as the context sequence length and batch size increase, the KV cache size is getting larger than LLM weights, urging the need for KV cache compression. Eigen Attention [19] has been proposed to compress the KV cache after applying RoPE but suffers a relatively large accuracy loss. To improve the accuracy, the most naive way is to compress the pre-RoPE KV cache. However, as Palu [4] points out, this will greatly introduce additional computation for recovering the key vectors. Palu further proposes the grouped-head low-rank decomposition optimization to reduce the computation overhead. We agree with Palu's observation but tackle the computation from the sparse perspective. By only selecting a subset of all the tokens (the critical tokens), the low-rank key vectors reconstruction complexity is greatly reduced. By integrating sparse attention, we observe that the KV cache size, data movement and computation complexity are all reduced as summarized in Table 1.

2.2 Sparse Attention

Early efforts to reduce attention complexity in transformers, such as Sparse Transformer [5], Reformer [12], and Longformer [3], primarily focused on training-based approaches to achieve sparse attention. In contrast, recent studies [17, 22, 33] have explored *post-training sparse attention*, leveraging the inherent sparsity of attention scores to identify the most salient tokens without retraining. For instance, StreamingLLM [26] identifies initial and recent tokens as critical, while others [32, 33] accumulate attention scores to locate important tokens in the KV cache. Quest [22] assesses KV cache page importance via min/max metrics, and Double-sparse [29] selects key KV tokens across important channels. However, most of these post-training approaches mainly reduce bandwidth and computation cost, leaving the KV cache uncompressed and thus a potential bottleneck [20, 28].

Natively Sparse Attention (NSA) [30] introduces a dynamic hierarchical sparse strategy combining coarse-grained token compression with fine-grained token selection. Unlike SALS, NSA requires training from scratch to learn a compressed attention module. In contrast, SALS can be calibrated *post-training*, performing top-k token selection based on low-rank latent approximations rather than a trained sparse module. This allows SALS to achieve comparable sparsity behavior without retraining and with precise control over the KV-cache compression process.

Overall, our work addresses the limitation of prior sparse attention methods by storing and operating on a low-rank KV cache, then selectively reconstructing high-dimensional representations for exact sparse attention. This design preserves accuracy while substantially reducing memory and computation overhead.

3 Challenges on Latent Space Transformation

In this section, we first review the RoPE mechanism preventing the fusion of query and key states in latent space. We also show that after RoPE, the key vector variance increases as well as the rank. We then analyze the pre-RoPE representational capability of tokens in the latent space, focusing on their ability to preserve key semantic features.

3.1 Latent Space Transformation with RoPE

The introduction of the RoPE mechanism complicates the low-rank transformation into the latent space. We begin by considering the case without RoPE. Let $\mathbf{K} \in \mathbb{R}^{s\times d}$ denote the key matrix, where s is the number of tokens and d is the dimensionality of each head. By applying an orthonormal projection matrix $\mathbf{U} \in \mathbb{R}^{d\times r}$, with $r \ll d$, we can transforme origin Key matrix into latent space:

$$\widetilde{\mathbf{K}} = \mathbf{K}\,\mathbf{U} \tag{1}$$

so that each original Key vector $\mathbf{k}_t \in \mathbb{R}^d$ is mapped to latent space $\widetilde{\mathbf{k}}_t \in \mathbb{R}^r$ leading to kv cache compression rate d/r. This method works well on the basis of that

$$\mathbf{U}\mathbf{U}^{\mathbf{T}} \approx \mathbf{I},\ \ \mathbf{Q}\mathbf{K}^{\mathbf{T}} \approx \mathbf{Q}\mathbf{U}\mathbf{U}^{\mathbf{T}}\mathbf{K}^{\mathbf{T}} \tag{2}$$

However, once RoPE is introduced, the relative order between the RoPE rotation matrix $\mathbf{R}$ and the lowrank projector $\mathbf{U}\mathbf{U}^\top$ becomes crucial. In Equation 3, we show both design choices in a single expression: (i) pre-RoPE transformation, where keys are first transformed and then rotated, and (ii) post-RoPE transformation, where keys are rotated first and transformed afterwards. For a query at position i and a key at position j, the attention score be approximated in two lowrank forms:

$$\mathbf{Q}_i\,\mathbf{K}_j^\top \;\approx\; \underbrace{\mathbf{Q}\,\mathbf{R}_i\big(\mathbf{R}_j^\top\,\mathbf{U}\mathbf{U}^\top\big)\,\mathbf{K}^\top}_{\text{pre-RoPE}} \quad \text{or} \quad \underbrace{\mathbf{Q}\,\mathbf{R}_i\big(\mathbf{U}\mathbf{U}^\top\,\mathbf{R}_j^\top\big)\,\mathbf{K}^\top}_{\text{post-RoPE}}, \tag{3}$$

where $\mathbf{R}_i$ and $\mathbf{R}_j$ are the RoPE rotation matrices for positions i and j, respectively.

Ideally, we can adopt the post-RoPE transformation to cache $\widetilde{\mathbf{K}} = \mathbf{K}\mathbf{R}_j\mathbf{U}$ and transform the rotated query into a latent space $\widetilde{\mathbf{Q}} = \mathbf{Q}\mathbf{R}_i\mathbf{U}$ to avoid the reconstruction complexity. However, as we will discuss later, applying RoPE will rotate the key vectors with larger variance, making them difficult to approximate using a low-rank matrix. On the other hand, in the pre-RoPE transformation, caching $\widetilde{\mathbf{K}}$ and reconstructing the full-rank keys as $\widetilde{\mathbf{K}}\mathbf{U}^\top$ will result in substantial overhead.

Variance amplification for post–RoPE rotation. Previous works [4, 20] observe that the key cache exhibits low-rank characteristics with a relatively small rank to retain approximately 90% of the energy. As such, we can use a single projection weight $\mathbf{U}$ as shown in Equation 1 to compress the key cache. However, we find that this phenomenon only holds for the key cache prior to applying RoPE. From Figure 1(b), we observe that applying RoPE to a set of key vectors pushes the data points outward and rotates their principal axes. As shown in Figure 1(b), the principal component is rotates away from its original direction and the points become more scattered with two main principal components. This indicates the increased rank due to applying RoPE. Moreover, the principal components rotate based on the token position, suggesting that a single fixed projection matrix may no longer approximate all of these rotated subspaces. Therefore, a pre–RoPE key for latent space transformation is preferable for maintaining accuracy.

Compute overhead during pre–RoPE reconstruction From Figure 1(a), we compare full attention with pre–RoPE low–rank compression across sequence lengths ranging from 1 K to 32 K tokens. While low–rank compression can reduce memory size, the time spent reconstructing low-rank keys/values from their rank-r form and applying the RoPE rotation grows linearly with sequence length and soon dominates the total attention runtime at 32 K tokens. This aligns with our analysis of Equation 3, which intruoduces a trade-off of memory savings and computational cost.

3.2 Token Representation in Latent Space

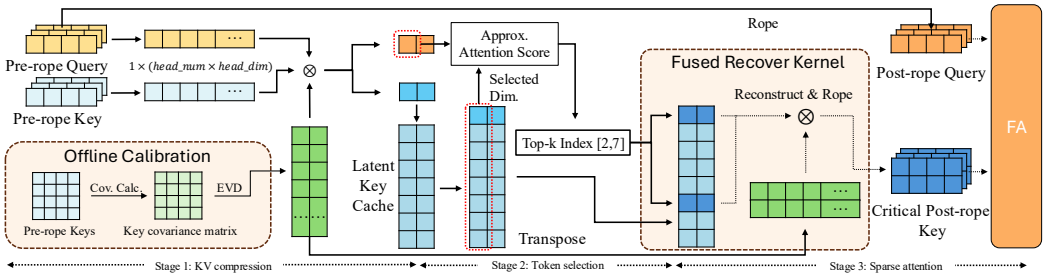

Figure 3: Overall architecture of SALS. Three stages are introduced with stage 1 for multi-head KV Cache compression, stage 2 for token selection in latent space and stage 3 for sparse attention.

To quantify the token representations of the query and key in the latent space, we first compute the latent-space attention vector $\tilde{\mathbf{p}} = \tilde{\mathbf{Q}}\tilde{\mathbf{K}}$, where in the pre-RoPE setting, $\tilde{\mathbf{Q}} = \mathbf{QU}$. Let $\mathcal{C} = \{i_1, i_2, \ldots, i_{N_c}\} \subseteq \{1, \ldots, s\}, \quad N_c \ll s$, denote the index set corresponding to the top-N_c entries of $\tilde{\mathbf{p}}$. The *overlap score (OS)* measures the token representation in the latent space, which is fraction of the full attention mass that these indices capture. $OS = \sum_{i \in \mathcal{C}} p_i / \sum_{i=1}^{s} p_i$, where p_i denotes the i-th entry of the full attention distribution $p \in \mathbf{R}^s$.

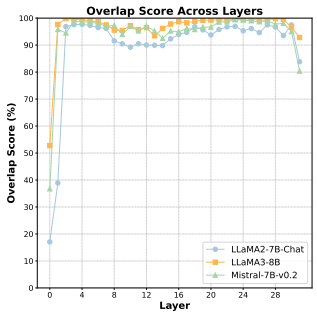

Figure 2: High overalp rate of pre-RoPE across layers

Figure 2 presents the overlap score for LLaMA–7B-chat, LLaMA–8B and Mistral-7B-v0.2. We observe that the average overlap score mostly remains above 90% for layers 2-29 but drops below 50% in layers 0, 1. A similar observation has been reported for hybrid RoPE attention design [27]. This finding indicates that, even when RoPE is completely omitted, latent space tokens can still preserve almost all of the full attention scores across the majority of layers.

4 Sparse Attention in Latent Space Framework

4.1 SALS Framework

In this section, we introduce our proposed SALS, which leverages a low-rank projection matrix to transform multi-head pre-RoPE keys into a compact single-head latent space, thereby markedly shrinking the memory footprint. To avoid the prohibitive cost of reconstructing the entire key cache, SALS estimates attention scores directly in the latent space, selects the top-N_c most critical tokens, and reconstructs only their corresponding keys. RoPE is only applied to the reconstructed keys, which are then used to compute the exact attention weights. Figure 3 provides a high-level summary of the SALS pipeline. Here, we use the top-k index $[2, 7]$ to indicate the selected tokens. The selected tokens are then reconstructed and reshaped to multi-head keys for sparse attention. The SALS framework is pipelined with three stages: KV cache compression to latent space, critical token selection in latent space and selective reconstruction from latent space for the later sparse attention.

4.2 Multi-head KV cache Compression to Latent Space

In the offline calibration process, we select a small calibration dataset from the pre-training corpus and collect its pre-RoPE key tensors. Let $\mathbf{K} \in \mathbb{R}^{s \times nd}$ denote the stacked multihead keys of the s calibration sequences. We begin by computing the empirical covariance of the calibration keys: $\mathbf{C} = \mathbf{K}^\top \mathbf{K}$. Applying an eigenvalue decomposition, $\mathbf{C} = \mathbf{U}\mathbf{\Sigma}\mathbf{U}^\top$, and selecting the leading r eigenvectors $\mathbf{U}_r$ yields the optimal rank-r projection matrix for the latent space. Note that the key vectors $\mathbf{K} \in \mathbb{R}^{s \times nd}$ are reshaped by merging the head number with head dimension. We provide the rational using the following lemma.

Lemma 1. *For any column-orthonormal matrix $\mathbf{U} \in \mathbb{R}^{h \times r}$ satisfying $\mathbf{U}^\top\mathbf{U} = \mathbf{I}_r$, we define the captured variance by $\mathbf{U}$ as $E(\mathbf{U})$. For the multi–head joint projection, all possible projection matrix set is defined as $\mathcal{U}_r := \{\mathbf{U} \in \mathbb{R}^{nd \times r} \mid \mathbf{U}^\top\mathbf{U} = \mathbf{I}_r\}$, and $\mathcal{B}_r := \{\mathrm{diag}(\mathbf{U}_1, \ldots, \mathbf{U}_n) \mid \mathbf{U}_i \in$*

Algorithm 1 Sparse Attention in Latent Space

Input: Pre-RoPE query $\mathbf{q} \in \mathbb{R}^{nd}$, key $\mathbf{k} \in \mathbb{R}^{nd}$, value $\mathbf{v} \in \mathbb{R}^{nd}$, Projection matrix $\mathbf{U}_r \in \mathbb{R}^{nd \times r}$, Low-rank key cache $\widetilde{\mathbf{K}} \in \mathbb{R}^{(S-1)\times r}$, quantised value cache $\widehat{\mathbf{V}} \in \mathbb{R}^{(S-1)\times nd}$, Sparsity budget k, Approx latent rank $r^\star$

Output: Attended output $\mathbf{y} \in \mathbb{R}^{nd}$

Function SPARSEATTENTION($\mathbf{q}, \mathbf{k}, \mathbf{v}, \mathbf{U}_r, \widetilde{\mathbf{K}}, \widehat{\mathbf{V}}, k$)
  $\tilde{\mathbf{q}} \leftarrow \mathbf{q}\mathbf{U}_r$; $\tilde{\mathbf{k}} \leftarrow \mathbf{k}\mathbf{U}_r$ # Project new token to r-dim. latent space
  $\widetilde{\mathbf{K}} \leftarrow \mathrm{concat}(\widetilde{\mathbf{K}}, \tilde{\mathbf{k}})$; $\widehat{\mathbf{V}} \leftarrow \mathrm{concat}(\widehat{\mathbf{V}}, \mathbf{v})$
  $\mathbf{p}' \leftarrow \tilde{\mathbf{q}}_{r^\star} \widetilde{\mathbf{K}}_{r^\star}^\top$ # Cheap similarity on top-$r^\star$ dims
  $\mathcal{C} \leftarrow \mathrm{TopK}(\mathbf{p}', k)$ # Selectr top–k critical token index
  $\mathbf{K}_\mathcal{C} \leftarrow \widetilde{\mathbf{K}}_\mathcal{C} \mathbf{U}_r^\top$ # Reconstruct critical latent key cache
  $\mathbf{q}^R \leftarrow \mathrm{RoPE}(\mathbf{q})$; $\mathbf{K}_\mathcal{C}^R \leftarrow \mathrm{RoPE}(\mathbf{K}_\mathcal{C})$ # Standard flash attention (FA) computation
  $\mathbf{p} \leftarrow \mathrm{softmax}\big(\mathbf{q}^R {\mathbf{K}_\mathcal{C}^R}^\top / \sqrt{d}\big)$
  $\mathbf{y} \leftarrow \mathbf{p}\, \widehat{\mathbf{V}}_\mathcal{C}$
  return $\mathbf{y}$
End Function

$\mathbb{R}^{d\times r'},\ \mathbf{U}_i^\top \mathbf{U}_i = \mathbf{I}_{r'}\}$, *where* $r' = r/n$*, is all possible projection matrix set for per–head projection. For all situations, the optimal* $\mathbf{U}$ *from multi–head joint projection matrix can capture more enery then per–head projection matrix:*

$$\max_{\mathbf{U}\in\mathcal{U}_r} E(\mathbf{U}) \ \geq \ \max_{\mathbf{U}\in\mathcal{B}_r} E(\mathbf{U})$$

Proof. Pick any $\mathbf{U} = \mathrm{diag}\big(\mathbf{U}_1, \ldots, \mathbf{U}_n\big) \in \mathcal{B}_r$ with $\mathbf{U}_i^\top \mathbf{U}_i = \mathbf{I}_{r'}$. Because the blocks occupy disjoint coordinate ranges, their product is blockdiagonal:

$$\mathbf{U}^\top \mathbf{U} = \mathrm{diag}\big(\mathbf{U}_1^\top \mathbf{U}_1, \ldots, \mathbf{U}_n^\top \mathbf{U}_n\big) = \mathrm{diag}(\mathbf{I}_{r'}, \ldots, \mathbf{I}_{r'}) = \mathbf{I}_r.$$

Hence $\mathbf{U}$ is column-orthonormal and thus $\mathbf{U} \in \mathcal{U}_r$; consequently $\mathcal{B}_r \subseteq \mathcal{U}_r$. Since every candidate in $\mathcal{B}_r$ is feasible for the joint search $\mathcal{U}_r$, maximizing over the larger set cannot yield a smaller value. □

4.3 Critical Token Selection in Latent Space

As discussed in previous works [25, 29], tokenwise attention is inherently sparse. However, identifying the relevant (*critical*) tokens fast enough remains the main bottleneck of most sparse-attention schemes. Guided by the observation in Sec 3.2 that pre-RoPE latent keys already reveal the sparsity pattern of the middle layers, we forgo the expensive full-rank query-key multiplication and instead work in the latent space.

More specifically, let $\mathbf{U}_r \in \mathbb{R}^{nd\times r}$ be the joint projector from Equation 1 and let $r^\star \ll r$ for scoring. We project the query once, $\tilde{\mathbf{q}} = \mathbf{U}_r^\top \mathbf{q} \in \mathbb{R}^r$, and keep only its leading coordinates $\tilde{\mathbf{q}}_{\,r^\star} \in \mathbb{R}^{r^\star}$. Each cached key already stores its full latent vector $\tilde{\mathbf{k}}_j = \mathbf{U}_r^\top \mathbf{k}_j$, from which we extract the first $r^\star$ dimensions, $\tilde{\mathbf{k}}_{j,:\,r^\star} \in \mathbb{R}^{r^\star}$. The approximate attention score of token in position j is a cheap inner product

$$s_j \ = \ \tilde{\mathbf{q}}_{:\,r^\star}^\top \, \tilde{\mathbf{k}}_{j,:\,r^\star}$$

Thus, critical tokens are identified directly from the existing key cache, without extra storage and at a fraction of the original compute.

4.4 Selective Reconstruction from Latent Space for Sparse Attention

Sparse attention is defined by restricting the standard attention computation to a selected subset of keys and values. Given a query matrix $\mathbf{Q} \in \mathbb{R}^{n\times d}$ and a full set of key and value matrices of length s, we identify a subset of salient indices

$$\mathcal{C} = \{i_1, i_2, \ldots, i_{N_c}\} \subseteq \{1, \ldots, s\}, \quad N_c \ll s, \tag{4}$$

where N_c denotes the number of selected positions on the token sequence. The corresponding submatrices $\mathbf{K}_{\mathcal{C}} \in \mathbb{R}^{N_c \times n \times d}$ and $\mathbf{V}_{\mathcal{C}} \in \mathbb{R}^{N_c \times n \times d}$ are extracted based on the selected indices$\mathcal{C}$. Here, the salient indices $\mathcal{C}$ are obtained via critical token selection in latent space. The sparse attention output is then computed by restricting the standard attention to the selected tokens:

$$\mathbf{p}_{\mathcal{C}} = \mathrm{softmax}\left(\frac{\mathbf{Q}\mathbf{K}_{\mathcal{C}}^{\top}}{\sqrt{d}}\right), \qquad \mathbf{y} = \mathbf{p}_{\mathcal{C}}\mathbf{V}_{\mathcal{C}}. \tag{5}$$

This method works well since the softmax operation normalizes the input distribution so that the output sums to 1 and only a few positions (or tokens) in $\mathcal{C}$ dominate with large values. The rest scores after softmax closes to 0. The whole SALS algorithm is summarized in Algorithm 1.

4.5 Performance Discussion

As the roofline model [8] suggests, the performance of a GPU is bounded by either computation or memory bandwidth. In attention computation, performance is commonly bounded by memory bandwidth [7], which is primarily consumed by KV cache data movement. For a context of s tokens and feature dimension d, full attention needs to transfer $2sd$ elements of keys and values. On the other hand, for the SALS framework, critical token selection and sparse attention both involve data movement. Critical token selection requires $r^{\star} \ll d$ latent dimensions, so the query–key dot products read $sr^{\star}$ elements. After selecting the top–k tokens, SALS only needs to access low-rank key and value caches, each of size kr. The second pass therefore moves $2kr$ elements.

Combining this two phases, the sparse variant moves $sr^{\star} + 2kr$ scalars, so its memory-bound speed-up is: $\frac{2sd}{sr^{\star}+2kr} = \frac{1}{d_{r^{\star}}/2 + d_r\, k_s}$. Here $d_{r^{\star}} = r^{\star}/d,\ d_r = r/d,\ k_s = k/s$ denote the latent-approximated-score ratio, the low-rank ratio, and the token sparsity, respectively. We develop a `Triton` kernel that fuses token selection, reconstruction and RoPE rotation into a single pass. This fused reconstruct–RoPE kernel reduces memory traffic by $7.69\times$ to $14.28\times$, depending on the chosen sparsity level and low-rank compression ratio, compared to the standard FlashAttention implementation.

5 Experiment

5.1 Setup

Models and tasks. We evaluate our SALS framework on two mainstream 7B chat models: LLaMA2–7B–Chat [23], that employs multi–head attention (MHA), and Mistral–7B–v0.2 [11], that uses grouped–query attention (GQA). To assess accuracy, we report results on the reasoning benchmark GSM8K [6], the conversational benchmark CoQA [16], and the 16 English subsets of LongBench [2] that probe long–context understanding. All experiments are conducted on a machine with Xeon(R) Platinum 8336C CPU, one GPU (ampere architecture), and 128G RAM.

Table 2: Evaluation on GSM8K and CoQA datasets for LLaMA2–7B–chat

Method	GSM8K (strict/flexible)↑	CoQA↑	Memory Access↓	Comp. ratio↓
baseline	0.2335 / 0.2335	0.5997	1.00	1.00
KIVI-4	0.2297 / 0.2305	0.5992	0.31	0.31
KIVI-2	0.2047 / 0.2047	0.6010	0.19	0.19
Palu-30%(3bit)	0.1713/0.1759	0.5938	0.14	0.14
Palu-50%(3bit)	0.0614/0.0879	0.5560	0.09	**0.09**
SALS-25%	**0.2312 / 0.2343**	0.5975	0.13	0.28
SALS-12.5%	0.2176 / 0.2229	**0.6070**	**0.07**	0.15

Baselines. We compare SALS with several state of the art baseline in two directions. For KV–cache compression we select Palu (low–rank projection) [4] and KIVI (quantization) [14]. For token–sparse decoding we include Double Sparse [29], Hshare [25], and Loki [20]. For the KV–cache compression baselines, we evaluate Palu at every reported compression ratio, including its variants that apply the optional quantisation step. For KIVI we evaluate both official settings: 4 bit and 2 bit. For the token–sparse baselines, sparsity is introduced only during the decoding phase, and we enforce the same overall sparsity ratio as Hshare to ensure a fair comparison.

Compression setup and calibration. To obtain the latent projection matrix, we randomly sample 512 sequences of length 4096 from the C4 corpus [9] and compute it offline. We apply multi-head *joint* compression to the key cache at two ratios: $d_r = 25\%$ and $d_r = 12.5\%$. For latent scoring,

Table 3: Evaluation on LongBench datasets

Model	Method	Single-QA	Multi-QA	Summarization	Few-shot	Synthetic	Code	Avg	Memory Access↓
LLaMA2-7B-chat	baseline	24.50	22.18	23.64	62.80	6.50	56.29	32.65	1.00
	KIVI-4bit	**24.76**	22.22	**23.40**	62.67	6.75	**56.42**	**32.70**	0.31
	Palu-30% (3bit)	22.36	22.01	22.66	60.39	**7.50**	50.53	30.91	0.13
	SALS-25%	24.37	**22.50**	**23.40**	**63.01**	6.50	53.80	32.26	**0.11**
	KIVI-2bit	23.11	21.40	22.67	62.81	**5.75**	**55.84**	31.93	0.19
	Palu-50% (3bit)	20.48	22.18	21.44	54.62	**5.75**	37.07	26.92	0.09
	SALS-12.5%	**24.81**	**22.52**	**23.08**	**62.84**	5.00	53.58	**31.97**	**0.06**
Mistral-7B-v0.2	baseline	36.43	29.65	28.06	66.72	44.87	52.96	43.12	1.00
	KIVI-4bit	36.34	29.85	**28.09**	**66.81**	**44.67**	**52.90**	**43.11**	0.31
	Palu-30% (3bit)	29.48	36.40	27.20	65.73	53.19	40.77	34.74	0.13
	SALS-25%	**36.61**	**29.92**	27.57	66.63	43.54	52.49	42.79	**0.11**
	KIVI-2bit	**35.34**	28.63	**27.72**	66.77	**39.68**	**52.63**	**41.80**	0.19
	Palu-50% (3bit)	26.73	**32.72**	25.73	63.25	18.57	44.43	35.71	0.09
	SALS-12.5%	35.18	29.88	27.18	**66.98**	35.32	51.39	40.99	**0.06**

we simply set $r^\star = 0.5r$ for all models. Since value tensors are almost full rank and play a pivotal role in attention, we forgo low-rank projection for them and instead perform *channel-wise group quantisation* that mirrors the key-cache setting (4 bit at 25% and 2 bit at 12.5%).

Following KIVI, we adopt a mixed high–precision / low–precision scheme: tokens in the most recent window are compressed by only 50%, whereas all preceding tokens are compressed according to the target ratio of the experiment. The high–precision window is aligned with the sparsity window: when the sparse mechanism always selects the most recent w tokens, the compression stage likewise keeps those same w tokens in high precision. Based on the observations in Figure 2, we skip the sparsification for layers 0, 1, and 31 across all models to ensure more accurate compression and sparsity results.

5.2 KVcache Compression Comparison

Implementation details. For the dataset GSM8K and CoQA, we always keep the most recent $w = 128$ tokens and decode the remaining context at a fixed sparsity of $1/4$. For the dataset LongBench, LLaMA2–7B–Chat supports a 4 k context window, whereas Mistral–7B–v0.2 supports 32 k. To equalise the average sparsity at $1/8$ on this benchmark, we retain $N_c = 512$ tokens for LLaMA2–7B–Chat and $N_c = 1024$ tokens for Mistral–7B–v0.2. For LLaMA2–7B–Chat we follow the Hshare [25] configuration ($x = 16$ sink tokens, $y = 432$ critical tokens, $z = 64$ recent tokens) and simply double each count for Mistral–7B–v0.2.

Results. Tables 2 shows the evaluation on the benchmark (GSM8K, CoQA) on LLaMA2–7B–chat model. We can see that although Palu achieves the highest compression rate, the acurracy drop is non-negligible, especillay for the GSM8K dataset. SALS provides two setting results with 25% KV cache compression rate (SALS–25%) and 12.5% compression rate (SALS–12.5%). SALS–25% achieves the best accuracy compared to KIVI and Palu, with neligible loss compared to the baseline. Tables 3 compares task-level performance across six LongBench categories, alongside normalized memory access costs. The first three columns reflect core reasoning tasks, where SALS achieves consistently strong performance. Notably, SALS-12.5% retains competitive accuracy while reducing memory access to just 6% of the baseline. This indicates that SALS preserves informative tokens more effectively. The memory-access savings translate into practical latency improvements, as fewer KV memory lookups reduce attention computation overhead.

5.3 Token-Sparse Comparison

Since SALS incorporates a sparsification stage, we also compare it with state of the art sparse decoders, such as Double Sparse, HShare and Loki in LongBench datasets.

Implementation details. We use the same sparse setting as Sec 5.2 for all methods, which have $x = 16$ sink tokens, $y = 432$ critical tokens and $z = 64$ recent tokens, achieving sparsity on LLaMA2–7b–chat at $1/8$.

Table 4: Comparison of Token Sparse Methods on `LLaMA2-7B-chat` Using LongBench Tasks

Method	Single-QA	Multi-QA	Summarization	Few-shot	Synthetic	Code	Avg	Memory Access↓
baseline	24.50	22.18	23.64	62.80	6.50	56.29	32.65	1.00
Double Sparse	24.78	**22.72**	**24.70**	61.84	4.17	51.66	31.64	0.16
HShare	24.59	22.18	24.54	61.69	4.74	53.26	31.83	0.14
Loki	24.57	18.09	24.37	**63.43**	4.75	56.49	31.95	0.19
SALS-25%	24.37	22.50	23.40	63.01	**6.50**	**53.80**	**32.26**	0.11
SALS-12.5%	**24.81**	22.52	23.08	62.84	5.00	53.58	31.97	**0.06**

Table 5: Performance comparison of baseline and SALS methods on the RULER dataset with Llama3.1-8B-Instruct (4k sequence length).

Method	avg	S1	S2	MK1	MK2	MV	MQ	FEW	QA1	QA2
Baseline	81.60	99.6	96.0	94.6	73.6	93.85	96.9	68.47	69.6	41.8
SALS-25%	80.81	99.6	95.2	94.2	65.8	93.2	96.4	71.53	70.2	41.2
SALS-12.5%	75.86	97.4	93.8	92.8	42.2	84.05	93.05	72.53	67.8	39.14

Result. Table 4 shows that, on LongBench, SALS with 25% key compression matches the average accuracy of the baseline while issuing only about 11% of the baselines memory traffic. When the compression is tightened to 12.5%, the Memory–Access Ratio drops to just 5.8%, yet SALS still outperforms all competing sparse methods in accuracy. These results suggest that the latent-space scoring mechanism selects critical tokens more accurately than existing heuristics, enabling KV-cache compression and token sparsity to coexist without loss of accuracy.

5.4 RULER Benchmark

Dataset. *RULER* [10] is a recently proposed long-context benchmark designed to evaluate the reasoning, retrieval, and compositional understanding capabilities of large language models across a wide range of input lengths and retrieval patterns. It decomposes the evaluation into fine-grained retrieval types, including *single-key*, *multi-key*, *multi-value*, and *multi-query* tasks, along with few-shot and question-answering (QA) subtasks. Compared with LongBench, RULER provides a more detailed breakdown of retrieval behaviors, making it well-suited for assessing token selection accuracy and KV-cache compression performance.

Implementation details. The experimental setup follows the same configuration as in Sec. 5.2. We evaluate all methods on a 128k-token context, applying an $8\times$ sparsity ratio, i.e., selecting 16k active tokens during inference. The retained-to-pruned token ratio is identical to that used in the LongBench experiments, ensuring consistent compression levels and comparable evaluation metrics. All experiments are conducted on the **LLaMA 3.1–8B–Instruct** model with a 4k sequence length.

Result. Table 5 summarizes the performance of SALS on the RULER dataset. At a 25% compression ratio, SALS achieves nearly identical average accuracy to the baseline (80.81 vs. 81.60), demonstrating its high fidelity in token selection and KV-cache reconstruction. Performance remains consistent across most retrieval subtasks, including *NIAH-Single-1/2*, *Multi-Value*, and *Multi-Query*, indicating that latent-space sparsification preserves key contextual semantics even under substantial cache reduction.

When the compression is further tightened to 12.5%, accuracy degradation mainly occurs in *NIAH-Single-1* and *Multi-Key-2*, where the retrieval dependency is strongest. Nevertheless, the model still achieves competitive overall performance (75.86 average) and stable scores on *Few-shot* and *QA* tasks. These results suggest that the proposed latent-space attention mechanism can maintain accurate token importance estimation even under extreme sparsity, enabling effective KV-cache compression with minimal accuracy loss across retrieval-oriented benchmarks.

5.5 Efficiency Evaluation

Inference details. Following Hshare [25], all speed tests are performed on the PyTorch backend, with the Triton–based fused kernel as discussed in Sec 4.5. We evaluate two aspects: *(i)*

Table 6: Attention Operator Latency (ms) across Methods and Input Configurations

Config (ms)	Flash-attn [7]	Loki [20]	Double-sparse [29]	Hshare [25]	SALS-25%	SALS-12.5%
bs=8, 1k	0.230	0.248	0.138	0.134	0.409 ± 0.093	0.357 ± 0.051
bs=8, 2k	0.830	0.464	0.237	0.430	0.430 ± 0.018	0.359 ± 0.012
bs=8, 4k	1.630	1.102	0.724	0.576	0.530 ± 0.008	0.439 ± 0.016
bs=16, 1k	0.440	0.452	0.223	0.134	0.415 ± 0.008	0.360 ± 0.011
bs=16, 2k	1.630	0.864	0.434	0.246	0.552 ± 0.040	0.444 ± 0.019
bs=16, 4k	3.230	2.101	1.319	1.067	0.757 ± 0.026	0.565 ± 0.013

self–attention latency and *(ii)* end–to–end generation speed–up. Self–attention latency is compared against FlashAttention–v2 [7], whereas end–to–end throughput is benchmarked against GPT–Fast [13]. Experiments use batch sizes of 8 and 16 and sequence lengths of $1\,\text{k}$, $2\,\text{k}$, and $4\,\text{k}$ tokens; the sparsity ratio is fixed at $1/8$ for all methods.

Result. Tables 6 reports our attention latency comparisons. Mean and varaince are reported using 1000 repetions. Thanks to the added token sparsity, SALS accelerates the standalone attention operator by $7,46\times$ speedup for batch size (bs) =8 and 4k sequence length (4k). Similar performance speed is also observed when batch size is 16. SALS will introduce some overhead for short sequences (e.g. 1k) but for longer sequences the speed-up is significantly better than the state-of-the-art sparse algorithm. As discussed in Section 4.5, reducing memory access will improve the attention performance.

Table 7 shows the end-to-end throughput speed-up of SALS comparing to the GPT-Fast results. Note that batch size is chosen 4 for sequence 64k to avoid GPU out of memory. Mean and varaince are reported using 50 repetions. We observe that when sequence is 8k, the speed-up of SALS-12.5% is $2.13\times$ although the sparsity ratio is 1/8. This is due to the overhead of reconstructing the selected token. When the sequence is set 32k, the speed-up of SALS-12.5% is increasing and reaches $4.57\times$. Coupled with the strong accuracy of SALS, these results confirm that combining latentspace KVcache compression with token sparsification offers an effective tradeoff between speed and accuracy.

Table 7: Long Context End-to-End Performance Throughput Comparison (token/second)

Bsz	Seq (k)	GPT-Fast	SALS-25%	SALS-12.5%
8	4	118	154.1 ± 7.1	163.5 ± 5.1
8	8	70.6	128.6 ± 5.1	150.1 ± 3.3
8	16	38.3	102.5 ± 0.3	122.7 ± 7.7
8	32	19.8	67.97 ± 0.8	89.47 ± 1.4
4	64	9.2	32.92 ± 0.3	42.96 ± 0.9

6 Conclusion

This paper investigates the KV cache compression based on the low-rank characteristics in the hidden dimension. We further discuss the increasing variance of keys due to applying rotary position embedding and propose to use the pre-RoPE keys to select the critical tokens. We observe that after the key vectors are transformed into the latent space, they largely maintain their representation across most layers and thereby the salient tokens are selected with high accuracy. Based on these insights, we propose the Sparse Attention in Latent Space (SALS) framework. The SALS framwork achieves compressed KV cache to the latent space, selects the critical token in the latent space with significantly less computation load and performs sparse attention on the selected tokens. By reconstructing only a small subset of important tokens, it avoids the overhead of full KV cache reconstruction. Experimental results demonstrate that SALS achieves SOTA performance by maintaining competitive accuracy under different settings and achieving 6.4-fold KV cache compression and 5.7-fold speed-up in attention compared to FlashAttention2 on 4K sequences. For the end-to-end throughput performance, we achieve 1.4-fold and 4.5-fold improvement compared to GPT-fast on 4k and 32K sequences respectively.

Acknowledgment

This work is supported by the National Nature Science Foundation of China (No. 62376020) and the Fundamental Research Funds for the Central Universities (No. 2025JBZY011).

References

[1] Anthropic. Claude. Large language model, May 2023. URL `https://www.anthropic.com/claude`. Accessed May 5, 2025.

[2] Y. Bai, X. Lv, J. Zhang, H. Lyu, J. Tang, Z. Huang, Z. Du, X. Liu, A. Zeng, L. Hou, et al. Longbench: A bilingual, multitask benchmark for long context understanding. *arXiv preprint arXiv:2308.14508*, 2023.

[3] I. Beltagy, M. E. Peters, and A. Cohan. Longformer: The long-document transformer. *arXiv preprint arXiv:2004.05150*, 2020.

[4] C.-C. Chang, W.-C. Lin, C.-Y. Lin, C.-Y. Chen, Y.-F. Hu, P.-S. Wang, N.-C. Huang, L. Ceze, M. S. Abdelfattah, and K.-C. Wu. Palu: Compressing kv-cache with low-rank projection. *arXiv preprint arXiv:2407.21118*, 2024.

[5] R. Child, S. Gray, A. Radford, and I. Sutskever. Generating long sequences with sparse transformers. *arXiv preprint arXiv:1904.10509*, 2019.

[6] K. Cobbe, V. Kosaraju, M. Bavarian, M. Chen, H. Jun, L. Kaiser, M. Plappert, J. Tworek, J. Hilton, R. Nakano, et al. Training verifiers to solve math word problems. *arXiv preprint arXiv:2110.14168*, 2021.

[7] T. Dao. Flashattention-2: Faster attention with better parallelism and work partitioning. *arXiv preprint arXiv:2307.08691*, 2023.

[8] N. Ding and S. Williams. *An instruction roofline model for gpus*. IEEE, 2019.

[9] I. Habernal, O. Zayed, and I. Gurevych. C4corpus: Multilingual web-size corpus with free license. In *Proceedings of the Tenth International Conference on Language Resources and Evaluation (LREC'16)*, pages 914–922, 2016.

[10] C.-P. Hsieh, S. Sun, S. Kriman, S. Acharya, D. Rekesh, F. Jia, Y. Zhang, and B. Ginsburg. Ruler: What's the real context size of your long-context language models?, 2024. URL `https://arxiv.org/abs/2404.06654`.

[11] A. Q. Jiang, A. Sablayrolles, A. Roux, A. Mensch, B. Savary, C. Bamford, D. S. Chaplot, D. d. l. Casas, E. B. Hanna, F. Bressand, et al. Mixtral of experts. *arXiv preprint arXiv:2401.04088*, 2024.

[12] N. Kitaev, Ł. Kaiser, and A. Levskaya. Reformer: The efficient transformer. *arXiv preprint arXiv:2001.04451*, 2020.

[13] P. Labs. gpt-fast: Simple and efficient pytorch-native transformer text generation in <1000 loc of python, 2023. URL `https://github.com/pytorch-labs/gpt-fast`. Accessed: 2025-05-14.

[14] Z. Liu, J. Yuan, H. Jin, S. Zhong, Z. Xu, V. Braverman, B. Chen, and X. Hu. Kivi: A tuning-free asymmetric 2bit quantization for kv cache. *arXiv preprint arXiv:2402.02750*, 2024.

[15] OpenAI. Chatgpt. Large language model, May 2023. URL `https://chat.openai.com/`. Accessed May 5, 2025.

[16] S. Reddy, D. Chen, and C. D. Manning. Coqa: A conversational question answering challenge. *Transactions of the Association for Computational Linguistics*, 7:249–266, 2019.

[17] L. Ribar, I. Chelombiev, L. Hudlass-Galley, C. Blake, C. Luschi, and D. Orr. Sparq attention: Bandwidth-efficient llm inference. *arXiv preprint arXiv:2312.04985*, 2023.

[18] R. Saha, N. Sagan, V. Srivastava, A. Goldsmith, and M. Pilanci. Compressing large language models using low rank and low precision decomposition. *Advances in Neural Information Processing Systems*, 37:88981–89018, 2024.

[19] U. Saxena, G. Saha, S. Choudhary, and K. Roy. Eigen attention: Attention in low-rank space for kv cache compression. *arXiv preprint arXiv:2408.05646*, 2024.

[20] P. Singhania, S. Singh, S. He, S. Feizi, and A. Bhatele. Loki: Low-rank keys for efficient sparse attention. *arXiv preprint arXiv:2406.02542*, 2024.

[21] J. Su, M. Ahmed, Y. Lu, S. Pan, W. Bo, and Y. Liu. Roformer: Enhanced transformer with rotary position embedding. *Neurocomputing*, 568:127063, 2024.

[22] J. Tang, Y. Zhao, K. Zhu, G. Xiao, B. Kasikci, and S. Han. Quest: Query-aware sparsity for efficient long-context llm inference, 2024.

[23] H. Touvron, T. Lavril, G. Izacard, X. Martinet, M.-A. Lachaux, T. Lacroix, B. Rozière, N. Goyal, E. Hambro, F. Azhar, et al. Llama: Open and efficient foundation language models. *arXiv preprint arXiv:2302.13971*, 2023.

[24] X. Wang, Y. Zheng, Z. Wan, and M. Zhang. Svd-llm: Truncation-aware singular value decomposition for large language model compression. *arXiv preprint arXiv:2403.07378*, 2024.

[25] H. Wu, L. Li, H. Huang, T. Yi, J. Zhang, M. Yu, and J. Yan. Hshare: Fast llm decoding by hierarchical key-value sharing. In *The Thirteenth International Conference on Learning Representations*, 2025.

[26] G. Xiao, Y. Tian, B. Chen, S. Han, and M. Lewis. Efficient streaming language models with attention sinks. *arXiv preprint arXiv:2309.17453*, 2023.

[27] B. Yang, B. Venkitesh, D. Talupuru, H. Lin, D. Cairuz, P. Blunsom, and A. Locatelli. Rope to nope and back again: A new hybrid attention strategy. *arXiv preprint arXiv:2501.18795*, 2025.

[28] D. Yang, X. Han, Y. Gao, Y. Hu, S. Zhang, and H. Zhao. Pyramidinfer: Pyramid kv cache compression for high-throughput llm inference. *arXiv preprint arXiv:2405.12532*, 2024.

[29] S. Yang, Y. Sheng, J. E. Gonzalez, I. Stoica, and L. Zheng. Post-training sparse attention with double sparsity. *arXiv preprint arXiv:2408.07092*, 2024.

[30] J. Yuan, H. Gao, D. Dai, J. Luo, L. Zhao, Z. Zhang, Z. Xie, Y. X. Wei, L. Wang, Z. Xiao, Y. Wang, C. Ruan, M. Zhang, W. Liang, and W. Zeng. Native sparse attention: Hardware-aligned and natively trainable sparse attention, 2025. URL `https://arxiv.org/abs/2502.11089`.

[31] Z. Yuan, Y. Shang, Y. Song, Q. Wu, Y. Yan, and G. Sun. Asvd: Activation-aware singular value decomposition for compressing large language models. *arXiv preprint arXiv:2312.05821*, 2023.

[32] T. Zhang, J. Yi, Z. Xu, and A. Shrivastava. Kv cache is 1 bit per channel: Efficient large language model inference with coupled quantization. *arXiv preprint arXiv:2405.03917*, 2024.

[33] Z. Zhang, Y. Sheng, T. Zhou, T. Chen, L. Zheng, R. Cai, Z. Song, Y. Tian, C. Ré, C. Barrett, et al. H2o: Heavy-hitter oracle for efficient generative inference of large language models. *Advances in Neural Information Processing Systems*, 36, 2024.

NeurIPS Paper Checklist

1. **Claims**

   Question: Do the main claims made in the abstract and introduction accurately reflect the paper's contributions and scope?

   Answer: [Yes]

   Justification: The abstract and introduction in this paper accurately reflect the papers contributions and scope.

   Guidelines:

   - The answer NA means that the abstract and introduction do not include the claims made in the paper.
   - The abstract and/or introduction should clearly state the claims made, including the contributions made in the paper and important assumptions and limitations. A No or NA answer to this question will not be perceived well by the reviewers.
   - The claims made should match theoretical and experimental results, and reflect how much the results can be expected to generalize to other settings.
   - It is fine to include aspirational goals as motivation as long as it is clear that these goals are not attained by the paper.

2. **Limitations**

   Question: Does the paper discuss the limitations of the work performed by the authors?

   Answer: [Yes]

   Justification: We discuss the limitation our method in the experiment section. Result is shown in Table 5 and discuss in Line 303.

   Guidelines:

   - The answer NA means that the paper has no limitation while the answer No means that the paper has limitations, but those are not discussed in the paper.
   - The authors are encouraged to create a separate "Limitations" section in their paper.
   - The paper should point out any strong assumptions and how robust the results are to violations of these assumptions (e.g., independence assumptions, noiseless settings, model well-specification, asymptotic approximations only holding locally). The authors should reflect on how these assumptions might be violated in practice and what the implications would be.
   - The authors should reflect on the scope of the claims made, e.g., if the approach was only tested on a few datasets or with a few runs. In general, empirical results often depend on implicit assumptions, which should be articulated.
   - The authors should reflect on the factors that influence the performance of the approach. For example, a facial recognition algorithm may perform poorly when image resolution is low or images are taken in low lighting. Or a speech-to-text system might not be used reliably to provide closed captions for online lectures because it fails to handle technical jargon.
   - The authors should discuss the computational efficiency of the proposed algorithms and how they scale with dataset size.
   - If applicable, the authors should discuss possible limitations of their approach to address problems of privacy and fairness.
   - While the authors might fear that complete honesty about limitations might be used by reviewers as grounds for rejection, a worse outcome might be that reviewers discover limitations that aren't acknowledged in the paper. The authors should use their best judgment and recognize that individual actions in favor of transparency play an important role in developing norms that preserve the integrity of the community. Reviewers will be specifically instructed to not penalize honesty concerning limitations.

3. **Theory assumptions and proofs**

   Question: For each theoretical result, does the paper provide the full set of assumptions and a complete (and correct) proof?

Answer: [Yes] ,

Justification: In this paper, all proofs of theorems are provided and all assumptions are clearly stated or referenced in the statement of any theorems

Guidelines:

- The answer NA means that the paper does not include theoretical results.
- All the theorems, formulas, and proofs in the paper should be numbered and cross-referenced.
- All assumptions should be clearly stated or referenced in the statement of any theorems.
- The proofs can either appear in the main paper or the supplemental material, but if they appear in the supplemental material, the authors are encouraged to provide a short proof sketch to provide intuition.
- Inversely, any informal proof provided in the core of the paper should be complemented by formal proofs provided in appendix or supplemental material.
- Theorems and Lemmas that the proof relies upon should be properly referenced.

4. **Experimental result reproducibility**

Question: Does the paper fully disclose all the information needed to reproduce the main experimental results of the paper to the extent that it affects the main claims and/or conclusions of the paper (regardless of whether the code and data are provided or not)?

Answer: [Yes]

Justification: All the settings are clearly discussed and cited. The results in this paper can be reproduced.

Guidelines:

- The answer NA means that the paper does not include experiments.
- If the paper includes experiments, a No answer to this question will not be perceived well by the reviewers: Making the paper reproducible is important, regardless of whether the code and data are provided or not.
- If the contribution is a dataset and/or model, the authors should describe the steps taken to make their results reproducible or verifiable.
- Depending on the contribution, reproducibility can be accomplished in various ways. For example, if the contribution is a novel architecture, describing the architecture fully might suffice, or if the contribution is a specific model and empirical evaluation, it may be necessary to either make it possible for others to replicate the model with the same dataset, or provide access to the model. In general. releasing code and data is often one good way to accomplish this, but reproducibility can also be provided via detailed instructions for how to replicate the results, access to a hosted model (e.g., in the case of a large language model), releasing of a model checkpoint, or other means that are appropriate to the research performed.
- While NeurIPS does not require releasing code, the conference does require all submissions to provide some reasonable avenue for reproducibility, which may depend on the nature of the contribution. For example
  (a) If the contribution is primarily a new algorithm, the paper should make it clear how to reproduce that algorithm.
  (b) If the contribution is primarily a new model architecture, the paper should describe the architecture clearly and fully.
  (c) If the contribution is a new model (e.g., a large language model), then there should either be a way to access this model for reproducing the results or a way to reproduce the model (e.g., with an open-source dataset or instructions for how to construct the dataset).
  (d) We recognize that reproducibility may be tricky in some cases, in which case authors are welcome to describe the particular way they provide for reproducibility. In the case of closed-source models, it may be that access to the model is limited in some way (e.g., to registered users), but it should be possible for other researchers to have some path to reproducing or verifying the results.

5. **Open access to data and code**

   Question: Does the paper provide open access to the data and code, with sufficient instructions to faithfully reproduce the main experimental results, as described in supplemental material?

   Answer: [Yes]

   Justification: : We provide open access to the data and code, with detailed instructions to reproduce all the experimental results.

   Guidelines:

   - The answer NA means that paper does not include experiments requiring code.
   - Please see the NeurIPS code and data submission guidelines (`https://nips.cc/public/guides/CodeSubmissionPolicy`) for more details.
   - While we encourage the release of code and data, we understand that this might not be possible, so No is an acceptable answer. Papers cannot be rejected simply for not including code, unless this is central to the contribution (e.g., for a new open-source benchmark).
   - The instructions should contain the exact command and environment needed to run to reproduce the results. See the NeurIPS code and data submission guidelines (`https://nips.cc/public/guides/CodeSubmissionPolicy`) for more details.
   - The authors should provide instructions on data access and preparation, including how to access the raw data, preprocessed data, intermediate data, and generated data, etc.
   - The authors should provide scripts to reproduce all experimental results for the new proposed method and baselines. If only a subset of experiments are reproducible, they should state which ones are omitted from the script and why.
   - At submission time, to preserve anonymity, the authors should release anonymized versions (if applicable).
   - Providing as much information as possible in supplemental material (appended to the paper) is recommended, but including URLs to data and code is permitted.

6. **Experimental setting/details**

   Question: Does the paper specify all the training and test details (e.g., data splits, hyperparameters, how they were chosen, type of optimizer, etc.) necessary to understand the results?

   Answer: [Yes]

   Justification: The paper details all the calibration and evaluation details necessary to understand the results.

   Guidelines:

   - The answer NA means that the paper does not include experiments.
   - The experimental setting should be presented in the core of the paper to a level of detail that is necessary to appreciate the results and make sense of them.
   - The full details can be provided either with the code, in appendix, or as supplemental material.

7. **Experiment statistical significance**

   Question: Does the paper report error bars suitably and correctly defined or other appropriate information about the statistical significance of the experiments?

   Answer: [Yes]

   Justification: For the speed-up experiment in our paper, we repeat the same setting for 10 times and report the average and varaince.For our benchmark accuracy, we do not repeat run the same benchmark multiple times since we notice very little variance in the accuracy.

   Guidelines:

   - The answer NA means that the paper does not include experiments.
   - The authors should answer "Yes" if the results are accompanied by error bars, confidence intervals, or statistical significance tests, at least for the experiments that support the main claims of the paper.

- The factors of variability that the error bars are capturing should be clearly stated (for example, train/test split, initialization, random drawing of some parameter, or overall run with given experimental conditions).
- The method for calculating the error bars should be explained (closed form formula, call to a library function, bootstrap, etc.)
- The assumptions made should be given (e.g., Normally distributed errors).
- It should be clear whether the error bar is the standard deviation or the standard error of the mean.
- It is OK to report 1-sigma error bars, but one should state it. The authors should preferably report a 2-sigma error bar than state that they have a 96% CI, if the hypothesis of Normality of errors is not verified.
- For asymmetric distributions, the authors should be careful not to show in tables or figures symmetric error bars that would yield results that are out of range (e.g. negative error rates).
- If error bars are reported in tables or plots, The authors should explain in the text how they were calculated and reference the corresponding figures or tables in the text.

8. **Experiments compute resources**

   Question: For each experiment, does the paper provide sufficient information on the computer resources (type of compute workers, memory, time of execution) needed to reproduce the experiments?

   Answer: [Yes]

   Justification: For each experiment, the paper provide sufficient information on the computer resources needed to reproduce the experiments

   Guidelines:

   - The answer NA means that the paper does not include experiments.
   - The paper should indicate the type of compute workers CPU or GPU, internal cluster, or cloud provider, including relevant memory and storage.
   - The paper should provide the amount of compute required for each of the individual experimental runs as well as estimate the total compute.
   - The paper should disclose whether the full research project required more compute than the experiments reported in the paper (e.g., preliminary or failed experiments that didn't make it into the paper).

9. **Code of ethics**

   Question: Does the research conducted in the paper conform, in every respect, with the NeurIPS Code of Ethics `https://neurips.cc/public/EthicsGuidelines`?

   Answer: [Yes]

   Justification: The research conducted in the paper conform, in every respect, with the NeurIPS Code of Ethics.

   Guidelines:

   - The answer NA means that the authors have not reviewed the NeurIPS Code of Ethics.
   - If the authors answer No, they should explain the special circumstances that require a deviation from the Code of Ethics.
   - The authors should make sure to preserve anonymity (e.g., if there is a special consideration due to laws or regulations in their jurisdiction).

10. **Broader impacts**

    Question: Does the paper discuss both potential positive societal impacts and negative societal impacts of the work performed?

    Answer: [Yes]

    Justification: The paper discusses the challenging problem of LLM long-context inference in the Introduction and the benefits to adopt our method. There is no negative societal impacts for the work.

Guidelines:

- The answer NA means that there is no societal impact of the work performed.
- If the authors answer NA or No, they should explain why their work has no societal impact or why the paper does not address societal impact.
- Examples of negative societal impacts include potential malicious or unintended uses (e.g., disinformation, generating fake profiles, surveillance), fairness considerations (e.g., deployment of technologies that could make decisions that unfairly impact specific groups), privacy considerations, and security considerations.
- The conference expects that many papers will be foundational research and not tied to particular applications, let alone deployments. However, if there is a direct path to any negative applications, the authors should point it out. For example, it is legitimate to point out that an improvement in the quality of generative models could be used to generate deepfakes for disinformation. On the other hand, it is not needed to point out that a generic algorithm for optimizing neural networks could enable people to train models that generate Deepfakes faster.
- The authors should consider possible harms that could arise when the technology is being used as intended and functioning correctly, harms that could arise when the technology is being used as intended but gives incorrect results, and harms following from (intentional or unintentional) misuse of the technology.
- If there are negative societal impacts, the authors could also discuss possible mitigation strategies (e.g., gated release of models, providing defenses in addition to attacks, mechanisms for monitoring misuse, mechanisms to monitor how a system learns from feedback over time, improving the efficiency and accessibility of ML).

11. **Safeguards**

    Question: Does the paper describe safeguards that have been put in place for responsible release of data or models that have a high risk for misuse (e.g., pretrained language models, image generators, or scraped datasets)?

    Answer: [NA]

    Justification: The paper has no such risks.

    Guidelines:

    - The answer NA means that the paper poses no such risks.
    - Released models that have a high risk for misuse or dual-use should be released with necessary safeguards to allow for controlled use of the model, for example by requiring that users adhere to usage guidelines or restrictions to access the model or implementing safety filters.
    - Datasets that have been scraped from the Internet could pose safety risks. The authors should describe how they avoided releasing unsafe images.
    - We recognize that providing effective safeguards is challenging, and many papers do not require this, but we encourage authors to take this into account and make a best faith effort.

12. **Licenses for existing assets**

    Question: Are the creators or original owners of assets (e.g., code, data, models), used in the paper, properly credited and are the license and terms of use explicitly mentioned and properly respected?

    Answer: [Yes]

    Justification: : The creators or original owners of assets used in the paper are properly credited and cited. The licenses and terms of use have been clearly mentioned and properly respected.

    Guidelines:

    - The answer NA means that the paper does not use existing assets.
    - The authors should cite the original paper that produced the code package or dataset.
    - The authors should state which version of the asset is used and, if possible, include a URL.

- The name of the license (e.g., CC-BY 4.0) should be included for each asset.
- For scraped data from a particular source (e.g., website), the copyright and terms of service of that source should be provided.
- If assets are released, the license, copyright information, and terms of use in the package should be provided. For popular datasets, `paperswithcode.com/datasets` has curated licenses for some datasets. Their licensing guide can help determine the license of a dataset.
- For existing datasets that are re-packaged, both the original license and the license of the derived asset (if it has changed) should be provided.
- If this information is not available online, the authors are encouraged to reach out to the asset's creators.

13. **New assets**

    Question: Are new assets introduced in the paper well documented and is the documentation provided alongside the assets?

    Answer: [Yes]

    Justification: The paper does not release new assets.

    Guidelines:

    - The answer NA means that the paper does not release new assets.
    - Researchers should communicate the details of the dataset/code/model as part of their submissions via structured templates. This includes details about training, license, limitations, etc.
    - The paper should discuss whether and how consent was obtained from people whose asset is used.
    - At submission time, remember to anonymize your assets (if applicable). You can either create an anonymized URL or include an anonymized zip file.

14. **Crowdsourcing and research with human subjects**

    Question: For crowdsourcing experiments and research with human subjects, does the paper include the full text of instructions given to participants and screenshots, if applicable, as well as details about compensation (if any)?

    Answer: [NA] .

    Justification: The paper does not involve crowdsourcing nor research with human subjects.

    Guidelines:

    - The answer NA means that the paper does not involve crowdsourcing nor research with human subjects.
    - Including this information in the supplemental material is fine, but if the main contribution of the paper involves human subjects, then as much detail as possible should be included in the main paper.
    - According to the NeurIPS Code of Ethics, workers involved in data collection, curation, or other labor should be paid at least the minimum wage in the country of the data collector.

15. **Institutional review board (IRB) approvals or equivalent for research with human subjects**

    Question: Does the paper describe potential risks incurred by study participants, whether such risks were disclosed to the subjects, and whether Institutional Review Board (IRB) approvals (or an equivalent approval/review based on the requirements of your country or institution) were obtained?

    Answer: [NA]

    Justification: The paper does not involve crowdsourcing nor research with human subjects.

    Guidelines:

    - The answer NA means that the paper does not involve crowdsourcing nor research with human subjects.

- Depending on the country in which research is conducted, IRB approval (or equivalent) may be required for any human subjects research. If you obtained IRB approval, you should clearly state this in the paper.
- We recognize that the procedures for this may vary significantly between institutions and locations, and we expect authors to adhere to the NeurIPS Code of Ethics and the guidelines for their institution.
- For initial submissions, do not include any information that would break anonymity (if applicable), such as the institution conducting the review.

16. **Declaration of LLM usage**

    Question: Does the paper describe the usage of LLMs if it is an important, original, or non-standard component of the core methods in this research? Note that if the LLM is used only for writing, editing, or formatting purposes and does not impact the core methodology, scientific rigorousness, or originality of the research, declaration is not required.

    Answer: [No]

    Justification: This paper is written by the authors and LLM is only used for grammar checking.

    Guidelines:

    - The answer NA means that the core method development in this research does not involve LLMs as any important, original, or non-standard components.
    - Please refer to our LLM policy (`https://neurips.cc/Conferences/2025/LLM`) for what should or should not be described.

A Key Dimensianlity Analysis with RoPE

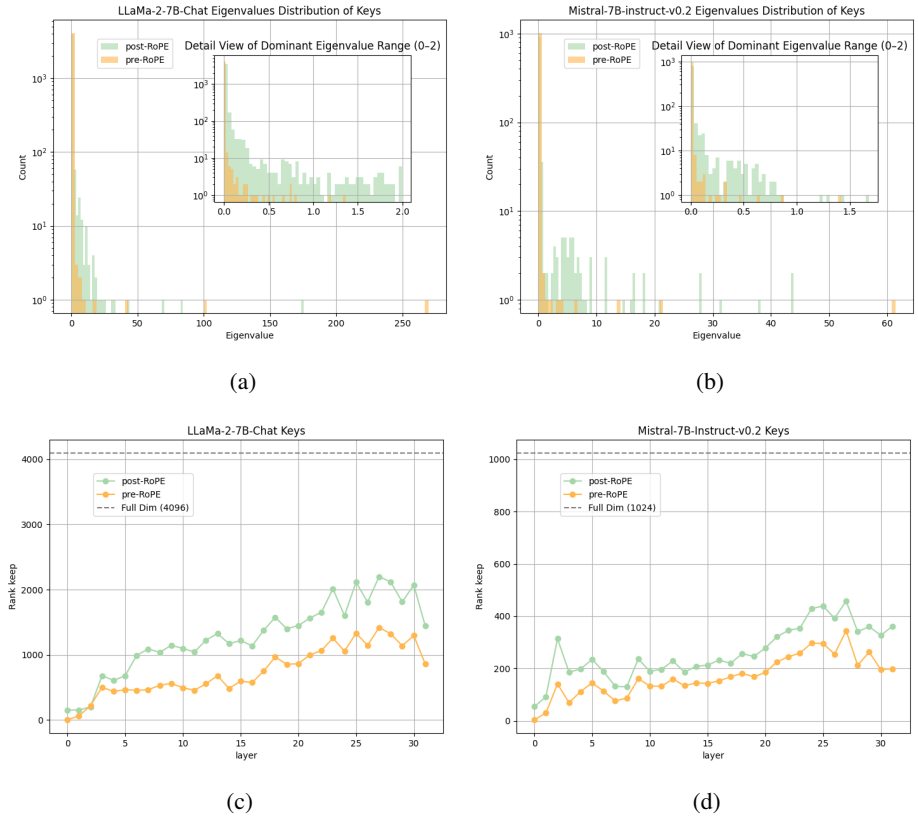

Figure 4: (a)–(b): Eigenvalue distributions of key covariance matrices in LLaMA-2-7B-Chat and Mistral-7B-Instruct-v0.2 before and after applying Rotary Position Embedding (RoPE). (c)–(d): Number of principal components required to retain 90% of the total variance across transformer layers, indicating changes in effective rank after RoPE.

In this section, we conduct a numerical analysis to quantify how rotary position embedding (RoPE) alters the principal-component structure of the key states. We perform principal component analysis (PCA) on the key tensors before and after applying RoPE, denoted as *pre-RoPE* and *post-RoPE*, respectively. Concretely, we first compute the covariance matrix of the key states and then carry out an eigenvalue decomposition. The magnitude of each eigenvalue reflects the contribution of its associated eigenvector: the presence of many small eigenvalues indicates that the corresponding representation is effectively low rank. To relate rank to the spectrum more systematically, we adopt the metrix introduced in Loki[20]:

$$\mathrm{Rank}_l(v) \;=\; \min\Big\{\, d \in \mathbb{Z}_+ : \sum_{i=1}^{d} \lambda_l^{(i)} \;\geq\; \frac{v}{100} \Big\},$$

where $\lambda_l^{(i)}$ denotes the i-th largest eigenvalue of the covariance matrix for the keys in layer l. This definition specifies the smallest number of principal components needed to explain at least $v\%$ of the total variance, enabling a direct comparison of the intrinsic dimensionality before and after RoPE.

Figure 4(a)–(b) illustrate the eigen–value spectra of the first layer ($l = 0$) for Llama–2–7B–Chat and Mistral–7B–Instruct–v0.2 under the pre–RoPE and post–RoPE conditions. The pre–RoPE spectra exhibit a markedly larger number of small eigenvalues, whereas the post–RoPE spectra are shifted upward, corroborating our earlier finding that RoPE increases the overall variance. Figure 4(c)–(d) present the layer–wise $\mathrm{Rank}_l(90)$ values, i.e. the minimal dimensionality needed to retain $90\,\%$ of the variance. For both models, the post–RoPE condition consistently requires a higher rank, reflecting the broader spectra observed in panels (a)–(b). In addition, the required rank varies substantially across layers, indicating that a layer–adaptive rank selection scheme could further enhance compression efficiency.